



50  
51  
52  
53  
54  
55  
56  
57  
58  
59  
60  
61  
62  
63  
64  
65  
66  
67  
68  
69  
70  
71  
72  
73  
74  
75  
76  
77  
78  
79  
80  
81  
82  
83  
84  
85  
86  
87  
88  
89  
90  
91  
92  
93  
94  
95

## Keywords

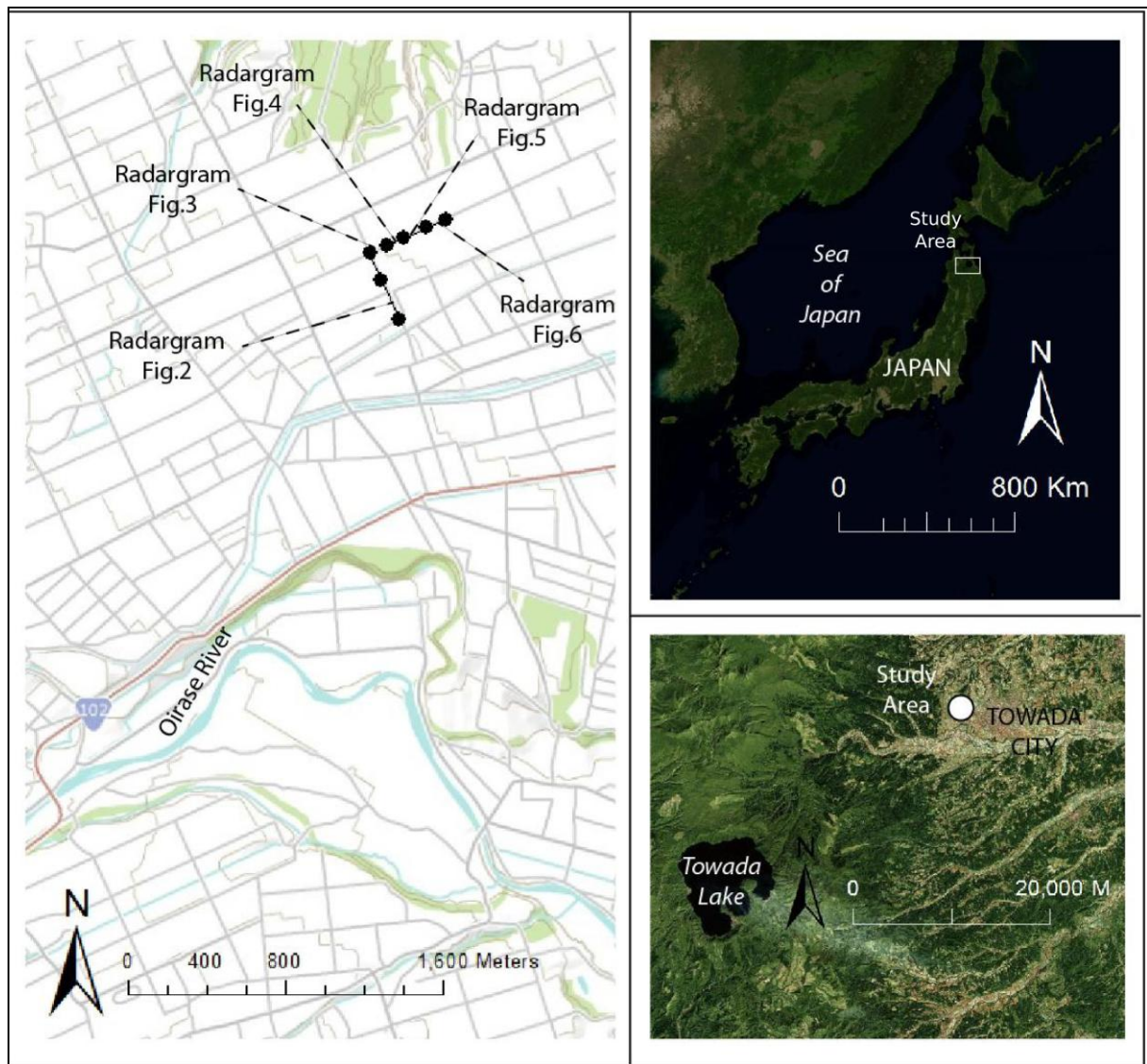
Towada Volcano; Aomori; Japan; Caldera; Sambongi fan; GPR; Ignimbrites; Outburst Flood

## 1. Introduction

Towada Volcano is located in between the provinces of Akita and Aomori, North-Honshu Island Japan (Fig. 1). Its summit reaches 915 m ASL (Above Sea Level), but the lake filling the summit caldera only reaches 400 m ASL. The caldera lake is 11 Km in diameter and has a surface of 61 km<sup>2</sup>. Within the 11 Km caldera, later Quaternary activity has produced a 2 Km wide caldera: the Nakanoumi caldera. On the rim of this second caldera, the Ogurayama dome has grown and can be seen emerging from the caldera lake. This lake of ~4.2 Km<sup>3</sup> (Kataoka, 2011) finds an exit in the Oirase River, flowing in a general Eastward direction to the Pacific Ocean, 70 Km from the outlet of the caldera lake.

Towada is an active volcano, with at least three major eruptive phases that created the present caldera, with the Okuse eruption 55 Ka, the Ofudo eruption 30 ka and the Hachinohe eruption 15 ka, which emplaced a large ignimbrite deposit incised by the Oirase river in its upper part. These deposits form the base of the Sambongi fan material studied in the present contribution, where the city of Towada presently extends. This geomorphologic feature of 17 Km long and 7 Km wide for a present area of 49 Km<sup>2</sup>, with an average gentle slope of 0.23 degrees has been named Sambongi fan (Nitobe, 1972) and Towada Terrace (Kudo, 2005). Kataoka (2011) follows the terminology Sanbongi fan, replacing the 'm' by 'n'. This difference is only a translation difference as the 'm' sound is a pronunciation variation of the same hiragana 'n' - like shimbashi = shinbashi for instance. According to Kataoka (2011), the low-gradient angle and the stacking patterns of the sediments of the Sambongi fan suggest that the sediments were emplaced by a watery, diluted flow close to hyperconcentrated flows, which lasted for a long period of time. These hyperconcentrated sheet-flows would have acted as conveyer belt, eventually carrying large blocks to the fan. Indeed, Kataoka (2011) has evidenced from outcrops and boreholes the presence of large blocks in the Sambongi fan (Towada Volcano, Japan). The size and the large amount of these blocks do not correspond with the river present competence, neither with the river estimated maximum palaeo-competence and neither to the fan gradient, therefore the author has concluded that the blocks have been emplaced by a large flood that partly created the deposit named 'Sambongi fan'.

Although these conclusions are based on several outcrops and a borehole, they are mostly concentrated on the margins of the deposits and along the present Oirase River and one still lack insights in the central part of the Sambongi fan, around Towada City. This lack of insight is due to the scarcity of natural outcrops in the Japanese Environment and the omnipresence of human activities hampering the direct access to sedimentary evidences.



96  
 97 *Fig. 1 Location of the Study area in North-Japan, Aomori Prefecture, between Towada*  
 98 *Lake - impounded in the caldera of the Towada Volcano - and Towada City. The 5*  
 99 *radargrams used in this study are located on the true left-bank of the Oirase River,*  
 100 *perpendicular (Radargram in Fig. 2) and parrallel (Radargrams in Fig. 3,4,5,6)*  
 101 *Oirase valley.*  
 102

103 Therefore, the present study's first objective is concerned with providing an insight of  
 104 the subsurface of the Sambongi fan - in large areas without any outcrops -, in order to  
 105 confirm or infirm the theory developed by [K.S. Kataoka \(2011\)](#). The second objective  
 106 focuses on the presence or not of blocks, because the distribution of blocks can help  
 107 understanding the flood processes depicted by [Kataoka \(2011\)](#): Was the energy mainly  
 108 concentrated in the present or a palaeo-valley or did the high-energy flow also fan over  
 109 a large area distributing boulders in a similar way, confirming K.S. Kataoka's theory?  
 110

111 To reach these objectives, this study has hence relied on GPR (Ground Penetrating  
 112 Radar). From the 1990s the usage of GPR in Earth-Sciences has been spreading widely  
 113 in areas as diverse as hydrostratigraphy ([e.g. Kostic et al., 2005](#)), landslide assessments  
 114 (e.g. [Grandjean et al., 2006](#)), faults identification ([e.g. Rashed et al., 2003](#)), etc. In  
 115 Volcanic and volcanic-derived terrain, one of the first study, by [Paillou et al. \(2001\)](#),

116 tested the applicability of GPR in volcanic dry terrain, however the results were  
117 spatially reduced to a 'borehole-like image' of the subsurface. The first extensive test of  
118 radargrams was conducted by Gomez-Ortiz et al. (2007) at Teide Volcano (Grand-  
119 Canaria); the authors have compared GPR radargrams against various materials  
120 outcrops: airfall deposits, massive-, heterogeneous lava, and flows dyke intrusions. This  
121 comparison has proven that the GPR is a suitable tool for the auscultation of volcanic  
122 subsurface, and more especially for the imaging of internal layers. This characterization  
123 calibrated against outcrops has also been accompanied by a contribution comparing  
124 Electric Resistivity and GPR derived data (Gomez-Ortiz et al., 2006). In Indonesia,  
125 historic (1815 AD) pyroclastic fall and flow deposits have been studied at Tambora  
126 Volcano (Abrams and Sigurdsson, 2007) and at Merapi Volcano for the 2006 eruption  
127 (Gomez et al., 2008, 2009). Although for older historic deposits, the study of the internal  
128 structure of pyroclastic-flow deposits was difficult to read on radargrams, this  
129 limitation has not been encountered on pristine block-and-ash flow deposits.  
130 Preliminary studies on lahar deposits at Mt. Semeru (East Java) have also been  
131 successful for the examination of internal structures down to 2 m depth, where the  
132 signal was perturbed by the water-table (Gomez and Lavigne, 2009). Carrivik et al.  
133 (2007) have also successfully imaged the sedimentary architecture of outburst flood  
134 deposits in Iceland with the aim of reconstructing the depositional regime.

## 135 136 137 **2. Methods**

138  
139 The dataset has been acquired on the Sambongi fan (Fig. 1), recording radargrams of a  
140 total length of 640. The GPR data has been recorded using a GPR Pulsekko-pro (owned  
141 by Tanaka-Corporation) mounted with 50 MHz antennas, which have a window of ~13  
142 m depth (theoretical optimum) and a vertical resolution of 0.5 m.

143 The data have been encoded based on the distance recorded from a coding-wheel on flat  
144 horizontal surfaces in order to ease the data processing. This encoding has been cross-  
145 correlated using the GPS GeoX 3.5G from Trimble (precision 10 cm in x,y during the  
146 acquisition with 9 to 12 satellites). The GPS data have been exported as shapefiles in the  
147 GIS solution of ESRI: ArcGIS 10®, in order to work on the distribution of the GPR data.  
148 The later has been processed with the software Reflex®. The generic processing is as  
149 follow: (1) Removal of Surface Echo; (2) Correction of Energy Decay; (3) 'Dewow'  
150 eliminating the mean on trace; (4) Correction of the AGC Gain; (5) Measure of the real  
151 velocities from blocks' hyperbolas and correction of the velocity accordingly (0.04 to  
152 0.075 m.ns-1 depending on the location) - since the study areas were flat, no further  
153 corrections were necessary.

154 Once the processing of the radargrams was completed, internal layers and punctual  
155 elements, such as blocks, were extracted, and the corresponding data were exported  
156 into GIS. It resulted in a series of radargrams of a total extend of 640 m, offering a wide  
157 window into the subsurface.

## 158 159 **3. Results**

### 160 161 **3.1 A Layering dominated by long sub-horizontal units**

162  
163 In this part, we have used the terms units and layers to identify units separated by  
164 linear reflectors, and we have also used the terms foresets and backsets in order to ease

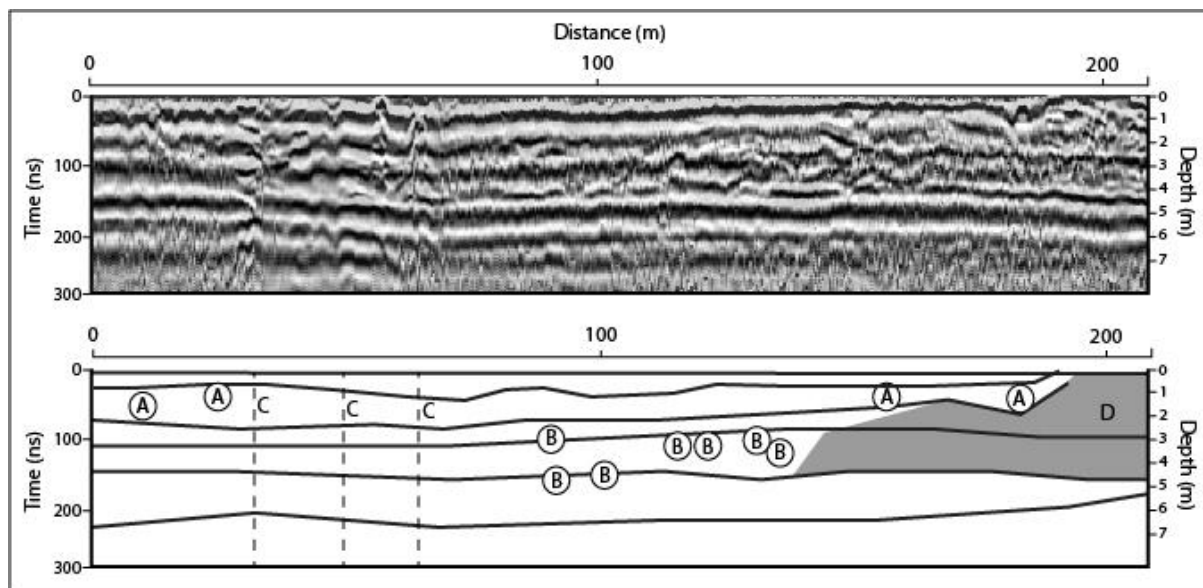
165 the explanation of the radargrams, however one must remember not to assimilate the  
 166 terms with sedimentary realms.

167  
 168 The studied area displays different patterns in the way the units are set together. The  
 169 internal layering is dominated by a subhorizontal layering with foresets, backsets, and  
 170 lenticular units.

171  
 172 On the radargram oriented perpendicularly to the Oirase Valley (Fig. 2), the dominating  
 173 pattern is a subhorizontal layering extending in a very regular manner, with little  
 174 thickness variations within the layers. On Fig. 2, we can distinguish at least 5 different  
 175 layers lying on a sole layer located between 5 and 7 m below the surface. This sole layer  
 176 has very different dielectric characteristics, as the GPR signal does not penetrate it at all.  
 177 The horizontal lines appearing within this lowest unit are echoes of the limits located  
 178 above. This difference between the sole layer and the 5 other layers on top is  
 179 characterized by a strong signal reflection.

180 The subhorizontal top layers are all at least 200 m long. The thickness of the layers is  
 181 comprised between 1 m and 3 m. They are perturbed by (c) (Fig.2) which are the results  
 182 of metallic elements located close to the surface, blocking the signal. During the data  
 183 collection, these elements have been recognized as water pipe-covers.

184 This horizontal layering has also been evidenced on the other radargrams (Fig. 3 to 6),  
 185 which are perpendicular to the first radargram, offering an image of the longitudinal  
 186 structure of the deposit.  
 187



188  
 189 *Fig. 2 A 200 m long radargram of a transversal section of the Southern extend of the*  
 190 *Sambongi fan (Location in Fig. 1, Radargram 1). Located between 3 and 5 m depth, the*  
 191 *punctual elements (A) are blocks, which are part of the deposits; punctual elements (B)*  
 192 *are located in the substratum above 2 m depth, therefore they could be the results of*  
 193 *anthropogenic activities; (C)s are perturbation in the signal created by reflectors close to*  
 194 *the surface; some contains iron and disturb all the imagery below; (D) is an area with a*  
 195 *large amount of punctual elements, which create a complex field of hyperbolas.*  
 196

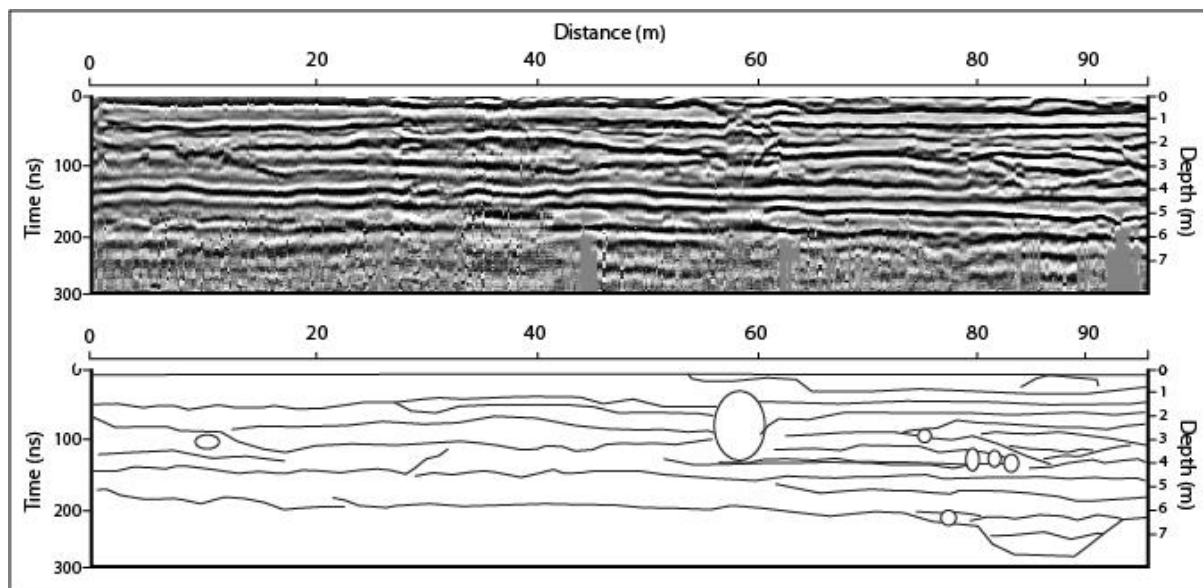
197 The 4 last radargrams present however more complexity than in Fig. 1. On Figure 3 and  
 198 4, the two first layers located below 5 m depth are regular sub-horizontal units, which  
 199 extend for at least 100 m length each. These layers could not be clearly accounted for on  
 200 the radargram of Fig. 5 and 6.

201 Lying on top of these two layers, there is an alternation of backsets and foresets  
 202 between ~3 and ~5 m depth. The foreset series is slightly dipping downstream: on Fig.  
 203 3 between 0 and 60 m, and on Fig. 4, between 0 and 40 m. The second series of units is  
 204 the backset, dipping downstream-ward. This backset bed dominates the radargrams in  
 205 Fig. 3,4 and 6. The backset is continuous from 60 m distance (Fig. 3) to the end of  
 206 radargram on Fig. 4 (~100 m length). On Radargram Fig. 5, there is a short foreset  
 207 intercalated between 0 and 30 m, before the bed displays a backset pattern until 120 m.  
 208 The backset units are not uniform; there are two main types: (1) short units of <10 m  
 209 length, with the all layer dipping in one direction (Fig. 4, between 50 and 75 m between  
 210 3 and 5 m depth; on Fig. 5 between 40 and 80 m, between 3 and 5 m depth); and (2)  
 211 long units of 10 m and more (e.g. Fig. 5 between 60 and 80 m).

212 These backsets are disturbed by elements such as lenses units and short foresets of  
 213 units on less than 10 m length (Fig. 3 Dist. 80 – 90 m; Fig. 4 Dist. ~20 m and Dist. ~40  
 214 m).

215 Located above the foreset and backset, one can find a series of long units, mostly  
 216 subhorizontal forming an underdeveloped backset. In this series of units located above  
 217 2 or 3 m depth, the irregularities recorded in the foreset below do not find any  
 218 repercussion, and all the units are very regular.

219  
 220



221  
 222 *Fig. 3: A 95 m long radargram (Location: Fig. 1; Radargram 2). The radargram is*  
 223 *dominated by subhorizontal layers and a series of shorter layers between 80 and 90 m.*  
 224 *The mark (A) around 60 m is created by the hole below a 'bridge', covered itself by soil of a*  
 225 *few tens of centimeter thick. There are very few punctual elements on this radargram.*  
 226

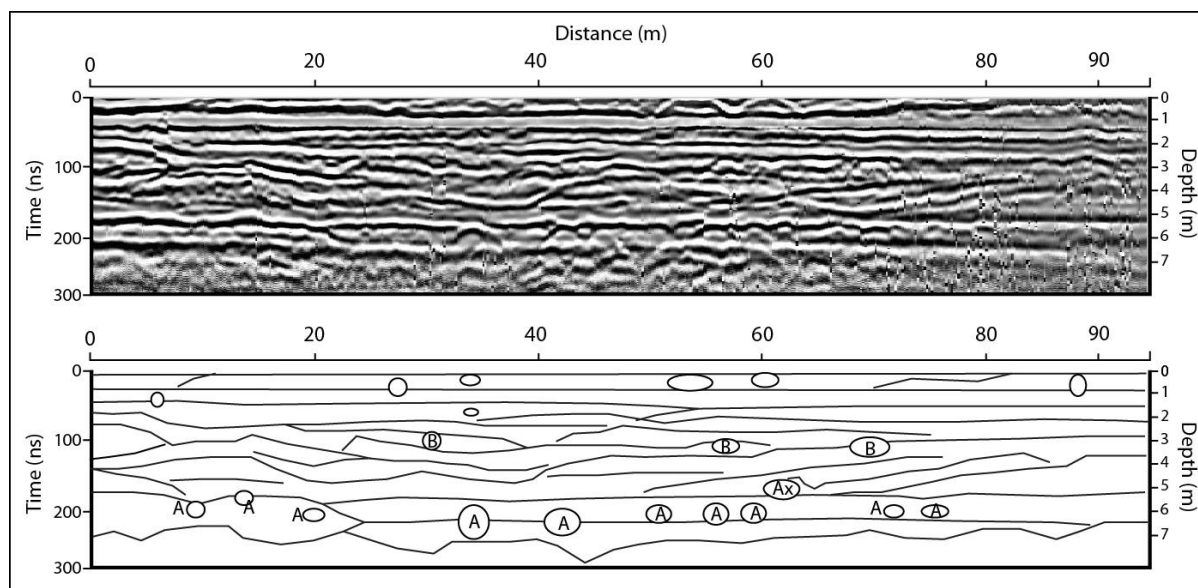


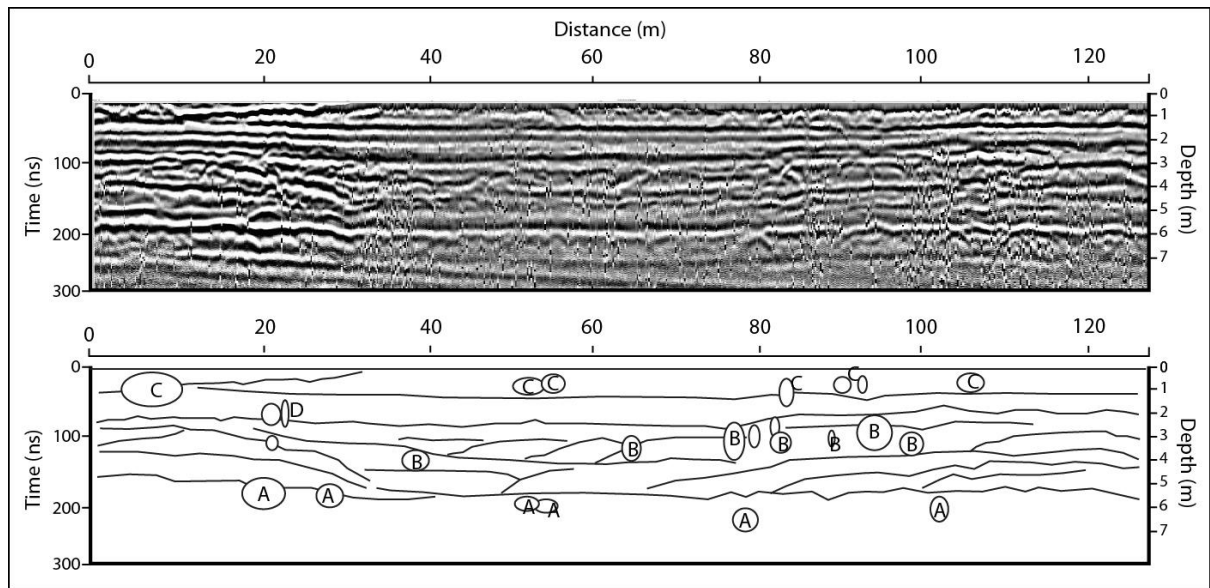
Fig. 4: A 95 m long radargram (Location: Fig.1 Radargram Fig. 4). The relatively complex layering is mixed with what appears to be at least two layers with blocks (As' and Bs'). Block between 1 m depth and the surface can't be confidently attributed to any 'natural' process, as they can have been emplaced by anthropogenic activity.

### 3.2 Examination of punctual reflectors in the deposit

One can notice the presence of punctual elements >50 cm diameter – minimum size detectable by the set of antenna used for the survey. The punctual elements are concentrated in 3 horizontal bands, which are constant on the 5 radargrams: (1) the first band is located below 5 m depth, at the upper limit of the lower unit, through which the GPR can't 'see'; (2) the second band is between 5 m and >2 m depth; (3) the third band is above 2 m depth, with most of the punctual reflectors above 1 m depth. We have recognized that the later punctual elements could have been emplaced by human activity, hence we did not include them in the interpretation.

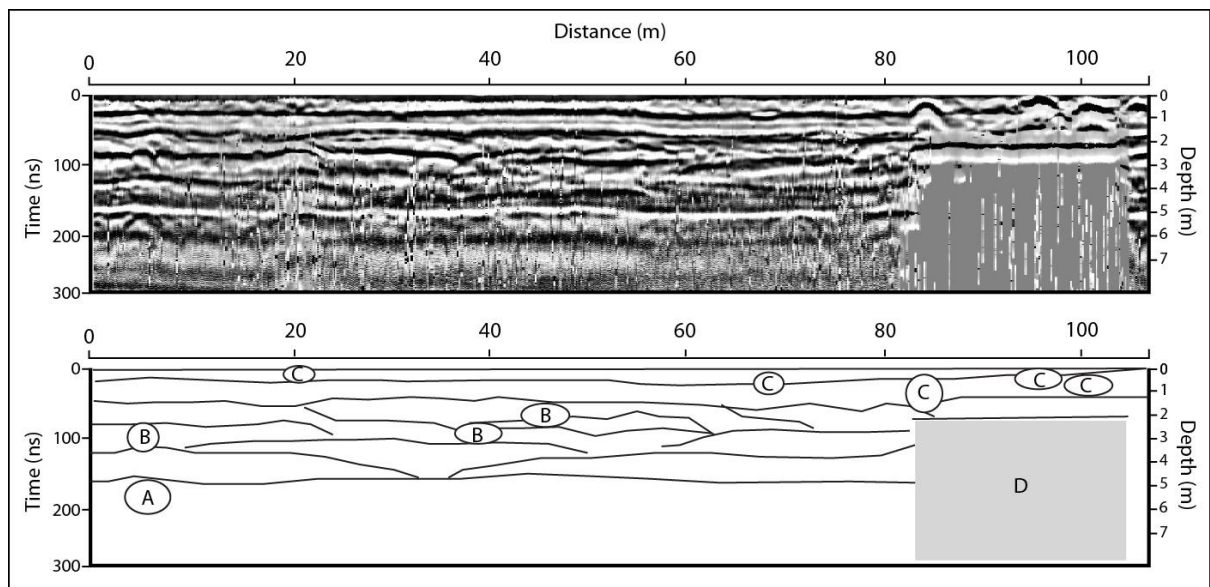
The punctual reflectors in the band (1) are all isolated elements, and they are distributed quite evenly along the radargrams. These punctual reflectors seem to sit on the lower unit, as they are all located precisely on the limit of the lower unit. Punctual reflectors of the band (2), located between 3 and 5 m depth, are more spread vertically and they can be isolated (e.g. blocks B of Fig. 6) or in cluster (e.g. blocks B of Fig. 5 between 50 and 100 m).

227  
228  
229  
230  
231  
232  
233  
234  
235  
236  
237  
238  
239  
240  
241  
242  
243  
244  
245  
246  
247  
248  
249  
250



251  
252  
253  
254  
255  
256  
257

*Fig. 5 Longitudinal transect of the Sambongi fan (Location in Fig. 1, Transect Fig. 5). (A) Punctual elements – most certainly blocks – located at the limit between the bottom unit and the other layers on top. (B) Blocks located in units between >2 and 5 m depth. (C) Blocks and punctual elements, which may have been emplaced by human activity.*



258  
259  
260  
261  
262  
263  
264  
265  
266  
267  
268  
269  
270

*Fig. 6 Fig. 5 Longitudinal transect of the Sambongi fan (Location in Fig. 1, Transect Fig. 6). (A) Punctual elements – most certainly blocks – located at the limit between the bottom unit and the other layers on top. (B) Blocks located in units between >2 and 5 m depth. (C) Blocks and punctual elements, which may have been emplaced by human activity. (D) Perturbation in the signal created by a linear (or planar in 3D) object emplaced at 2 m depth.*

#### 271 4. Interpretations and Discussion

272

273 The radargrams have revealed that a layered deposit of 5 to 7 m was lying over a unit of  
274 electromagnetically impenetrable material. The layers are generally subhorizontal, with  
275 regular latitudinal (perpendicular to the actual valley) extents that exceed 200 m. The 4  
276 radargrams, extending along the present valley, display more complexity; with a series  
277 of foresets and backsets and lensed-units located between 3 and 5 m depth. On top of  
278 this series and below, one can find long subhorizontal layers.

279 Within the deposits, there is also a high number of punctual reflectors, which are large  
280 blocks > 50 cm diameter (compared with the data of [Kataoka, 2011](#)) located into two  
281 depth-bands. The first set of blocks is located at the junction between the lowest unit –  
282 through which the GPR can't see through – and within the central units, between 3 and  
283 5 m. Punctual elements above 2 m aren't scarce either, but they could be of  
284 anthropogenic origin; therefore we did not work from them.

285 The units evidenced by GPR are by comparison with [Kataoka \(2011\)](#), as follow: a first  
286 layer of ignimbrite deposit located at the bottom, through which the radar could not see.  
287 From 5 to 7 m depth, on top of the ignimbrite deposits, a series of units more or less  
288 regular has been emplaced by hyperconcentrated-flow sheets. Above ~2 m depth, the  
289 soil layers haven't been part of the present study (GPR work at this depth requires a  
290 different set of antennas), and therefore won't be discussed here. The presence of  
291 punctual elements in the radargrams can also be assimilated to blocks, as per the  
292 description of the Sambongi fan ([Kataoka, 2011](#)).

293 Despite an excellent correspondence between the GPR data and the description of visual  
294 evidences given by Kataoka, the units located between 5-7 m and 2-3 m depth have  
295 displayed complexities, which require further discussion.

296

297 Compared to other volcanic flow deposits deposited in confined valleys, the GPR signal  
298 reveals a very different structure ([Gomez et al., 2008, 2009](#)) to block-and-ash flow  
299 deposits, which are characterized by backsets of short layers, symbol of the  
300 progradation of the flow units during emplacement. The foresets observed in Sambongi  
301 fan is characterized by layers, which are closer to the horizontal and longer. This  
302 pattern can be linked to the low-gradient topography on which the layers are emplaced  
303 and to the open-field setting, which allows a spread of the layers. The present data is  
304 closer to the lahar deposits surveyed by GPR at Semeru Volcano ([Gomez and Lavigne,  
305 2010](#)). Indeed the radargram [Fig. 2](#) is (at a different scale) similar to the longitudinal  
306 transect at Semeru Volcano, and the other transects ([Fig. 3,4,5 and 6](#)) have similarities  
307 with the transversal radargrams of Semeru Volcano. The Smabongi fan being an  
308 unconfined environment, this would suggest that the sheet-flows, described by [Kataoka  
309 \(2011\)](#), would have been characterized by tongues of higher velocity and energy  
310 draping unevenly the area. These differences would be reduced when reaching the  
311 edges of the fan, explaining the very regular sandy units. The higher energy flow-  
312 tongues may have look like the one observed in the Sendai plain during the 3.11.2011  
313 tsunami.

314 Such flow was only one part of the flow, which emplaced the backsets and foresets  
315 located between 5 m depth and 3 m depth. Before their arrival and after their flowage,  
316 flows of lesser energy and/or lower sediment concentration would have emplaced the  
317 long uniform units, which one can found below and above the previously depicted units.  
318 This theory is also sustained by the position of the blocks, which are located within the  
319 set of units emplaced between 5 m and 3 m depth.

320 Finally, it is interesting to note that the study of the sedimentary architecture of  
321 outburst flood eskers by GPR (Burke et al., 2010) has provided an internal architecture,  
322 which seems close to the one we have evidenced at Towada, with antidune cross-strata,  
323 subhorizontal plane beds, backset beds, foreset beds and boulder clusters; the  
324 processes that emplaced the present Sambongi fan may have been similar.

325  
326  
327

## 328 **5. Conclusion**

329

330 The present contribution has confirmed the phenomenology of the eruption of the  
331 15,000 years ago eruption of the Towada Volcano and the rapid construction of the  
332 Sambongi fan. It also confirmed the hints gathered from outcrops that the fan was build  
333 by a succession of sheet-flows. However, it also proved that despite the general  
334 homogeneity suggested by the outcrops and the present morphology, the outburst flow  
335 has certainly experienced different phases with increase and decrease in energy and  
336 sediment concentration, creating the 'channel-like' features, the foresets and the  
337 backsets. It is interesting to note that these features do not follow the present direction  
338 of the valley, and that they may have found some continuity to the North in the  
339 presently cultivated palaeo-channels.

340

341

## 342 **Acknowledgement**

343

344 The Research Centre for Natural Hazards and Disaster Recovery, University of Niigata  
345 has funded 75% of the research, and the University of Canterbury (New Zealand) has  
346 funded 25%. The authors also appreciate the help of Tanaka Corporation, which  
347 provided the GPR material. The authors are also indebt to two anonymous reviewers,  
348 who have improved the present manuscript and shared their ideas and  
349 recommendation. xxxxxxxx

350

## 351 **References**

352

353 Abrams, L.-J., Sigurdsson, H. 2007. Characterization of pyroclastic fall and flow deposits  
354 from the 1815 eruption of Tambora volcano, Indonesia using ground-penetrating radar.  
355 *Journal of Volcanology and Geothermal Research* 161, 352-361.

356

357 Burke, M.J., Woodward, J., Russell, A.J., Fleisher, P.J., Bailey, P.K., 2010. The sedimentary  
358 architecture of outburst flood eskers: A comparison of ground-penetrating radar data  
359 from Bering Glacier, Alaska and Skeidararjokull, Iceland. *GSA Bulletin* 122, 1637-1645.

360

361 Carrivick, J.L., Pringle, J.K., Russell, A.J., Cassidy, N.J. 2007. GPR-Derived Sedimentary  
362 Architecture and Stratigraphy of Outburst Flood Sedimentation within a Bedrock  
363 Valley System, Hraundalur, Iceland. *Journal of Environmental and Engineering  
364 Geophysics* 12, 127-143.

365

366 Gomez, C., Lavigne, F. 2010. Transverse architecture of lahar terraces, inferred from  
367 radargrams: preliminary results from Semeru Volcano, Indonesia. *Earth Surface  
368 Processes and Landforms* 35, 1116-1121.

369  
370  
371  
372  
373  
374  
375  
376  
377  
378  
379  
380  
381  
382  
383  
384  
385  
386  
387  
388  
389  
390  
391  
392  
393  
394  
395  
396  
397  
398  
399  
400  
401  
402  
403  
404  
405  
406  
407  
408  
409  
410  
411  
412  
413  
414  
415  
416  
417

Gomez, C., Lavigne, F., Lespinasse, N., Hadmoko, D.S., Wassmer, P. 2008. Longitudinal structur eof pyroclastic-flow deposits revealed by GPR survey at Merapi Volcano, Java, Indonesia. *Journal of Volcnaology and Geothermal Research* 176, 439-447.

Gomez, C., Lavigne, F., Hadmoko, D.S., Lespinasse, P., Wassmer. 2009. Block-and-ash flow deposition: A conceptual model from a GPR survey on pyroclastic-flow deposits at Merapi Volcano, Indonesia. *Geomorphology* 110, 118-127.

Gomez-Ortiz, D., Martin-Velazquez, S., Martin-Crespo, T., Marquez, A., Lillo, J., Lopez, I., Carreno, F., Martin-Gonzalez, F., Herrera, R., De Pablo, M.A. 2007. Joint application of ground penetrating radar and electrical resistivity imaging to investigate volcanic materials and structures in Tenerife (Canary Islands, Spain). *Journal of Applied Geophysics* 62, 287-300.

Gomez-Ortiz, D., Martin-Velazquez, S., Martin-Crespo, T., Marquez, A., Lillo, J., Lopez, I., Carreno, F. 2006. Characterization of volcanic materials using ground penetrating radar: a case study at Teide volcano (Canary Islands, Spain). *Journal of Applied Geophysics* 59, 63-78.

Grandjean, G., Pernetier, C., Bitri, A., Meric, O., Malet, J.-P. 2006. Caracterisation de la structure interne et de l'etat hydrique de glissements argilo-marneux par tomographie geophysique: l'exemple du glissement-coulee de Super-Sauze (Alpes du Sud, France). *Comptes Rendus de Geoscience* 338, 587-597.

Kataoka, K.S. 2011. Geomorphic and sedimentary evidence of a gigantic outburst flood from Towada caldera after the 15 ka Towada-Hachinohe ignimbrite eruption, northeast Japan. *Geomorphology* 125, 11-25.

Kostic, B., Becht, A., Aigner, T. 2005. A 3-D sedimentary architecture of a Quaternary gravel delta (SW-Germany): implications for hydrostratigraphy. *Sedimentary Geology* 181, 143-171.

Kudo, T., 2005. Geology of the Towada District. Quadrangle series, scale 1:50,000, Geological Survey of Japan, AIST, 79 p. (in Japanese with English abstract).

Nitobe, K., 1972. Geomorphological study of the terraces in the middle and lower reaches of the Oirase River. *Annals of the Tohoku Geographical Association* 24, 77-85 (in Japanese with English abstract).

Paillou, Ph., Grandjean, G., Malezieux, J.-M., Ruffie, G., Heggy, E., Piponnier, D., Dubois, P., Achache, J. 2001. Performances of Ground Penetrating Radars in arid volcanic regions: Consequences for Mars subsurface exploraion. *Geophysical Research Letters* 28-5, 911-914.

Rashed, M., Kawamura, D., Nemoto, H., Miyata, T., Nakagawa, K. 2003. Ground penetrating radar investigations accross the Uemachi fault, Osaka, Japan. *Journal of Applied Geophysics* 53, 63-75.